Numerical Simulation Study using the Explicit Finite

Difference Method for Petroleum Reservoir

Sri Feni Maulindani^{1*}; Andry Prima²; Jati Arie Wibowo³; Pauhesti Rusdi⁴; Harin Widiyatni⁵

1,2,4,5 Petroleum Engineering Departement, Faculty of Earth Technology and Energy,
Universitas Trisakti, Jakarta, Indonesia, 11440

3 Petroleum Engineering Departement, Faculty of Exploration and Production Technology,
Universitas Pertamina, Jakarta, Indonesia, 12220

¹sri.feni@trisakti.ac.id; ²andry.prima@trisakti.ac.id; ³jati.aw@universitaspertamina.ac.id; ⁴pauhesti@trisakti.ac.id; ⁵harin@trisakti.ac.id

Received: 14th September 2024/ Revised: 30th August 2025/ Accepted: 12th September 2025

How to Cite: Maulindani, S. F., Prima, A., Wibowo, J. A., Rusdi, P., & Widiyatni, H. (2025). Numerical simulation study using the explicit finite difference method for petroleum reservoir. *ComTech: Computer, Mathematics and Engineering Applications*, 16(2), 153–168. https://doi.org/10.21512/comtech.v16i2.12191

Abstract - The behavior of petroleum reservoirs is inherently complex, making it challenging to determine their performance for both single-fluid and multiphase production systems. To accurately estimate the recovery reserves of a reservoir, a comprehensive understanding of its geometry and internal flow characteristics is essential. Numerical simulation serves as a fundamental tool for reservoir engineers, offering an efficient and reliable method to predict reservoir mechanisms, evaluate pressure variations, and estimate in-place hydrocarbon yield. This study employs mathematical modeling concepts and numerical techniques to analyze the dynamic behavior of petroleum reservoir systems. A flow model based on Partial Differential Equations (PDEs), specifically the diffusivity equation for unsteady-state fluid flow in porous media, is developed and applied. The diffusivity equation is discretized and solved mathematically using the explicit finite difference method to approximate pressure distribution over time and space. The primary objective of this research is to investigate and analyze the pressure distribution that governs reservoir performance under varying conditions. Sensitivity analyses are conducted to evaluate the influence of grid spacing, time step, hydraulic diffusivity, and boundary conditions on pressure reservoir behavior within a Cartesian grid for a one-dimensional, single-phase reservoir. The findings are expected to provide insight into the relationship between reservoir properties and fluid dynamics, supporting improved prediction of reservoir behavior. Ultimately, this research contributes to the optimization of petroleum production strategies and

enhances the understanding of reservoir engineering processes through quantitative simulation.

P-ISSN: 2087-1244

E-ISSN: 2476-907X

Keywords: numerical simulation, diffusivity equation, explicit finite difference method

I. INTRODUCTION

The study of solving the diffusivity equation in reservoir simulation using the explicit method presents a practical approach for addressing Partial Differential Equations (PDEs) in numerical reservoir modeling through finite difference techniques. This explicit method is relatively straightforward to implement, as it involves one unknown variable (pn + 1) for the next time level and three known variables (pn) for the current time level. Reservoir engineers apply explicit methods to solve more complex PDEs under various reservoir conditions, including two-phase and multiphase flows, as well as unconventional reservoirs characterized by dual porosity and dual permeability. These methods are also used across one-dimensional (1D), two-dimensional (2D), and three-dimensional (3D) grids. This study focuses on a single-phase, onedimensional reservoir and employs a second-order PDE formulation. The solution is discretized using the explicit finite difference method, with two boundary conditions applied: a no-flow boundary condition and a specified boundary condition, where the pressure remains constant between the left and right boundaries.

The application of finite difference methods to solve PDEs continues to attract significant attention

*Corresponding Author 153

and remains an active area of research in reservoir engineering. Over the years, numerous scholars explore and refine these numerical techniques to enhance the accuracy and stability of reservoir simulations. A variety of solution approaches—including Explicit, Implicit, Implicit Pressure and Explicit Saturation (IMPES), and Fully Implicit methods—are applied to model petroleum reservoirs operating under single-phase or multiphase conditions. These methods are implemented using both Cartesian and cylindrical coordinate grids, allowing for flexible representation of different reservoir geometries and flow behaviors. (Sun & Ertekin, 2019).

Additionally, the Finite Difference (FD) approach finds extensive application in seismic exploration, particularly for forward modeling, imaging, and inversion processes (Liu & Luo, 2022). Researchers continue to refine this method to improve computational efficiency and accuracy in complex geological settings. Sun et al. (2019) develop a nonconformal hybrid Finite Difference Time Domain (FDTD) and Finite Element Time Domain (FETD) technique that introduces hybridization through a buffer zone, effectively enhancing the method's stability and adaptability for seismic simulations.

Furthermore, an investigation and analysis of the one-dimensional heat equation are carried out using appropriate initial and boundary conditions with both Forward Time Centered Space (FTCS) and Crank–Nicolson (CN) methods (Mojumder et al., 2023). These numerical techniques are widely applied due to their stability and accuracy in solving transient heat conduction problems, offering valuable insights into the temporal and spatial behavior of thermal diffusion. In addition, a new numerical solver is developed to simulate two-phase flow with phase change in porous media, utilizing the Finite Volume Method (FVM) to enhance computational precision and efficiency in modeling complex multiphase flow systems (Ghedira et al., 2025).

The higher-order partial differential equation functions as a second-order backward differentiation formula for the time derivative, employing a specific numerical technique to approximate nonlinear terms (Keita et al., 2021). A study investigates solutions to partial differential equations related to heat transfer, applying both explicit and implicit finite difference schemes to analyze their computational behavior and accuracy. This research examines various parameters that influence temperature distribution in slabs, considering both one-dimensional and twodimensional configurations (Adak, 2020; Aliyu et al., 2021). In addition, the finite difference method is used to analyze the combined thermal and flow characteristics of Boger nanofluid containing carbon nanotube materials, taking into account the effects of Cattaneo-Christov heat flux and thermal radiation (Raza & Wang, 2024). Furthermore, the influence of capillary pressure is evaluated in fully implicit finite difference simulations, focusing on water saturation behavior in two-phase systems within both

homogeneous and heterogeneous porous media in numerical reservoir models (Wang et al., 2020).

The higher-order finite element method is applied to model unsteady, incompressible, and inviscid two-phase flows, utilizing the level set method with Galerkin discretization and a new explicit projection method to solve the incompressible Euler equations, where pressure and velocity fields are treated separately (Salomon & Guilcher, 2024). A finite volume scheme is also employed to simulate twophase flows in non-homogeneous and non-isotropic two-dimensional petroleum reservoirs using the IMPES method (Contreras et al., 2021). Furthermore, a higher-order numerical approach predicts the position of the fluid front and mitigates front smearing in large grids, minimizing computational errors in injection scenarios within production reservoirs. This is achieved through a second-order finite volume method coupled with a linear programming technique for $C0_2$ injection modeling (Kvashchuk et al., 2023). Additionally, a fully implicit one-dimensional thermal compositional two-phase flow simulator is utilized to compute counter-current flow and gravitational segregation in wellbores, where the governing equations are discretized using the finite volume method (Nascimento et al., 2021).

Predicting pressure distribution in petroleum reservoirs is essential for effective evaluation and management, as pressure variations occur both spatially and temporally. A practical approach to addressing this challenge involves formulating fluid flow equations based on specific reservoir characteristics and solving them numerically using Explicit and Implicit finite difference methods (Appau et al., 2019). These numerical techniques enable reservoir engineers to simulate complex flow behaviors, assess reservoir performance, and make informed decisions regarding production optimization and recovery efficiency.

The block-centered grid and point-distributed grid are the two most widely used formats for representing petroleum reservoirs in numerical simulations. In a point-distributed grid, the boundary grid lies along the reservoir boundary, while grid points representing boundary blocks are positioned midway between the interior and the boundary (Abou-Kassem et al., 2020). These grid systems provide flexible spatial discretization, enabling accurate modeling of pressure and saturation variations across the reservoir.

Recently, a new method for simulating unconventional reservoirs containing incompressible fluids has been developed to address two-phase systems, particularly oil and water, in non-isotropic two-dimensional reservoirs. This approach utilizes a finite volume quadrilateral grid to discretize pressure, ensuring numerical stability and spatial accuracy. Additionally, a high-resolution Correction Procedure via Reconstruction (CPR) scheme is implemented for discretizing saturation, improving the precision of fluid front prediction and minimizing numerical diffusion (Galindez-Ramirez et al., 2020).

This study employs commercial CMG-IMEX

software to perform reservoir simulations, focusing on black oil models characterized by dual porosity, radial grid flow, and single-phase reservoir conditions. The objective is to evaluate pressure distribution and fluid flow performance under varying parameters of fractured reservoirs (Maulindani et al., 2021). Further research extends this analysis by examining dual-porosity reservoir behavior through a type curve analytical solution approach, demonstrating a strong correlation between numerical reservoir simulations and analytical model predictions (Maulindani et al., 2021).

Based on the reviewed literature, the present study aims to determine the pressure distribution in a petroleum reservoir by solving the Diffusivity Equation using the explicit finite difference method. This approach is applied to a one-dimensional single-phase reservoir model formulated on a Cartesian coordinate grid. The analysis investigates reservoir behavior through a simplified numerical framework, emphasizing the sensitivity of grid spacing, time steps, hydraulic diffusivity, and boundary conditions in influencing pressure performance and overall reservoir dynamics.

II. METHODS

The research methodology applied in examining the diffusivity equation follows the framework established by Sun and Ertekin (2019). In this study, an explicit one-dimensional single-phase approach is utilized for reservoir simulation. The fundamental differential equations governing pressure transient analysis are formulated in Equation (2), while the reservoir simulation process is represented in Equation (1), each expressed in different coordinate systems to accommodate varying reservoir geometries and flow conditions.

$$\frac{\partial^2 P}{\partial x^2} = \frac{\emptyset \mu c}{k} \frac{\partial P}{\partial t} \tag{1}$$

$$\frac{\partial^2 p}{\partial r^2} + \frac{1}{r} \frac{\partial p}{\partial r} = \frac{\phi \mu C}{k} \frac{\partial p}{\partial t} \tag{2}$$

Equations (1) and (2) represent the coupling of three fundamental fluid flow principles in porous media, collectively referred to as the diffusivity equations. Numerous researchers have applied these equations to analyze and predict fluid flow behavior in petroleum reservoirs under various geological and operational conditions. The third fundamental principle, the conservation of mass—also known as the continuity equation—approximates the inflow and outflow rates within porous media, as shown in Equation (3). Furthermore, Darcy's Law, which characterizes the mechanism of fluid flow through porous structures, is presented in Equation (4). The equation of state for slightly compressible fluids, which relates pressure and fluid density variations, is expressed in Equation (5).

$$(v_x \rho_x \Delta y \Delta z) - (v_{x + \Delta x} \rho_{x + \Delta x} \Delta y \Delta z) \, = \, (\Delta x \Delta y \Delta z) \emptyset \, \frac{(\rho_{t + \Delta t} - \rho_t)}{\Delta t}$$

$$v = -\frac{k}{\mu} \frac{\partial P}{\partial x} \tag{3}$$

$$c = \frac{1}{\rho} \frac{\sigma \rho}{\partial P} \tag{5}$$

The finite difference method is applied to discretize the diffusivity equation into a numerical derivative form, emphasizing variations in pressure and time. This process utilizes the central difference approximation derived from the Taylor series expansion (Sun & Ertekin, 2019). Through the application of the Taylor series, forward and backward difference equations are systematically derived to approximate the temporal and spatial derivatives. Equation (6) illustrates the forward difference formulation, while Equation (7) presents the corresponding backward difference expression.

$$P(x + \Delta x) = p(x) + \Delta x p'(x) + \frac{1}{2} \Delta x^2 p'(x) + \frac{1}{6} \Delta x^3 p'(x)$$
(6)

$$p(x - \Delta x) = p(x) - \Delta x p'(x) + \frac{1}{2} \Delta x^2 p'(x) - \frac{1}{6} \Delta x^3 p'(x)$$
(7)

The first derivative solution obtained using the forward finite difference approach is presented in Equation (8), while the backward finite difference formulation for the first derivative is shown in Equation (9). By subtracting Equation (9) from Equation (8), the central finite difference approximation for the first derivative is derived, as expressed in Equation (10). This central finite difference provides improved accuracy by averaging the effects of the forward and backward approximations, thereby reducing numerical error in the derivative estimation.

$$p'(x) = \frac{p(x-\Delta x) - p(x)}{\Delta x} + O(\Delta x)$$
(8)

$$p'(x) = \frac{p(x) - p(x + \Delta x)}{\Delta x} + O(\Delta x)$$
(9)

$$p'(x) = \frac{p(x+\Delta x) - (x-\Delta x)}{\Delta x} + O(\Delta x^2)$$
(10)

The errors associated with these finite difference approximations vary between the forward, backward, and central schemes. The forward and backward schemes exhibit truncation errors of order Δx , whereas the central difference scheme achieves higher accuracy with errors of order Δx^2 . These truncation errors arise from approximating the continuous partial differential equation using discrete numerical formulations, reflecting the degree of precision inherent in each finite difference method.

By adding Equation (6) and Equation (7), the resulting expression is presented in Equation (11). Solving for $p'^{(x)}$ provides the second derivative

finite difference, as shown in Equation (12). The truncation error associated with this second derivative approximation is of the order Δx^2 demonstrating greater numerical accuracy compared to first-order schemes. The diffusivity Equation (1) is subsequently solved using the Explicit finite difference method, as expressed in Equation (13).

$$p(x + \Delta x) + p(x - \Delta x) = 2p(x) + \Delta x^2 p''(x) + 0(\Delta x^4)$$
(11)

$$p'^{\prime(x)} = \frac{p(x+\Delta x)-2p+p(x-\Delta x)}{\Delta x^2} + O(\Delta x^2)$$
 (12)

$$\frac{p_{i+1}^{n} - 2p_{i}^{n} + p_{i-1}^{n}}{\Delta x^{2}} = \frac{\phi \mu c_{t}}{k} \frac{p_{i}^{n+1} - p_{i}^{n}}{\Delta t}$$
(13)

Hydraulic diffusivity, denoted as γ , is a physical parameter that characterizes the behavior of fluid flow within porous media. It is governed by the diffusivity equation, which defines the manner in which pressure varies spatially and temporally throughout the reservoir. This variation is influenced by the intrinsic properties of both the reservoir rock and the fluid as they interact over time. Hydraulic diffusivity determines the rate at which pressure disturbances propagate through the formation, serving as a critical factor in understanding and predicting reservoir fluid dynamics.

Higher hydraulic diffusivity within the reservoir allows for a more rapid response to variations in oil well injection or production rates. Hydraulic diffusivity is defined as the ratio involving permeability, porosity, viscosity, and compressibility, which collectively influence the fluid flow characteristics of the reservoir. This relationship is mathematically expressed in Equation (1). Subsequently, the pressure distribution for the next time level is determined, as presented in Equation (15), with the parameter α defined in Equation (16).

$$\gamma = \frac{\phi \mu c_t}{k} \tag{14}$$

Where,

 $\phi = porosity$

 $\mu = viscosity$

 $c_t = compressibility total$

k = permeability

$$P_i^{n+1} = \alpha p_{i+1}^n + (1 - 2\alpha) p_i^n + \alpha p_{i-1}^n$$
 (15)

$$\alpha = \frac{\Delta t}{\Delta x^2 \gamma} \tag{16}$$

Where,

 α = Alpha

 Δt = Time step

 Δx^2 = Grid space

γ = Hydraulic Diffusivity

Numerical stability is a fundamental aspect of reservoir simulation, directly associated with the

accuracy and performance of the diffusion equation. This equation is utilized to determine dependent parameters, including the reservoir model and its physical properties. In this process, the spatial and temporal derivatives are approximated using a truncated Taylor series expansion. The resulting truncation error emerges from this approximation, as computational systems can only handle a finite number of digits when solving the finite difference equation. Consequently, the numerical solution obtained differs from the exact analytical solution of the partial differential equation (Sun & Ertekin, 2019).

To minimize truncation error and enhance the accuracy of the numerical approximation, the discrepancy between a partial differential equation and its finite difference representation at a specific point in space and time within the domain must be reduced. This discrepancy is referred to as the local truncation error or local discretization error. Accordingly, the truncation error, denoted as ε_{Li}^n , is expressed in Equation (17). The diffusivity Equation (1) can then be examined alongside its corresponding finite difference approximation in Equation (13), which defines the local truncation error at the discrete spatial point i and time level n, as shown in Equation (18).

$$\varepsilon_{Li}^{n} = \left| f_{fd} \right|_{i}^{n} - \left| f_{d} \right|_{i}^{n} \tag{17}$$

$$\epsilon_{Li}^{n} = \left[\frac{p_{i+1}^{n} - 2p_{i}^{n} + p_{i-1}^{n}}{\Delta x^{2}} = \frac{\phi\mu c_{t}}{k} \frac{p_{i}^{n+1} - p_{i}^{n}}{\Delta t}\right] - \left(\frac{\partial^{2}P}{\partial x^{2}}\right] = \frac{\phi\mu c}{k} \frac{\partial P}{\partial t} \Big|_{i}^{n}$$

$$\tag{18}$$

The local truncation error in Equation (10) cannot be precisely quantified because it involves the subtraction of terms expressed in algebraic (discrete) and continuous forms. Consequently, the solution derived from the finite difference (discrete) method does not fully converge to the exact solution of the differential problem, even when the grid dimensions are significantly reduced. This condition exemplifies a round-off error, which can rapidly dominate the intended solution and lead to inaccurate computational results.

To ensure convergence, conducting a stability analysis of the numerical approximation is essential. This analysis is crucial because finite difference schemes can exhibit varying stability characteristics—being unconditionally stable, conditionally stable, or unconditionally unstable. The most widely used approach for evaluating the stability of such schemes is the von Neumann, or Fourier, analysis. This method assesses the growth or decay of initial errors in the finite difference approximation by expressing them as a finite Fourier series, as represented in Equation (19).

$$\sum_{n} A_{n} e\left(\frac{\ln \pi x}{L}\right) \tag{19}$$

In this context, l is $\sqrt{-1}$, and l denotes the interval over which the function is defined. The Fourier

series method utilizes nodes derived from the solution, which can be expressed as a product of spatial and time-dependent terms. Furthermore, according to this method, the numerical scheme remains stable as long as the amplification factor, denoted as μ_{max} , is less than one. The mathematical expression for the amplification factor is presented in Equation (20).

$$\mu_{max} = \left(\frac{|\xi^{n+1}|}{|\xi^n|}\right)_{max} \tag{20}$$

The stability analysis for the convergence of the one-dimensional diffusivity equation using the explicit scheme is presented in Equation (21). The explicit finite difference method remains stable only when specific conditions defined by this equation are satisfied, indicating that the scheme is conditionally stable. In this method, the solution for an unknown point at a given time step is computed directly from the known values at preceding time steps. This process is illustrated in Figure 1 (see Appendices), which provides a schematic representation of the solution framework in the explicit finite difference method.

$$\frac{\Delta t}{\Delta x^2 \gamma}$$
 < 0.5 (21)

The solution to the diffusivity equation in numerical simulations depends on two fundamental conditions: the initial condition and the boundary condition. The initial condition, such as the reservoir pressure, provides the necessary starting point for accurately modeling reservoir behavior. Boundary conditions include both inner boundaries, which define parameters like flow or injection rates, and outer boundaries, which play a crucial role in constraining and guiding the overall simulation process.

In the context of outer boundary conditions, two primary types are commonly applied in reservoir simulations. The first is the no-flow boundary, which typically occurs at the corners of the reservoir model or grid block. This condition is defined by a zero pressure gradient across the boundary, meaning that no fluid crosses it. In unsteady-state scenarios, it is referred to as a Neumann-type boundary condition. The second type is the Dirichlet-type boundary condition, which applies to boundaries where a specific pressure value is maintained. This condition represents a constant-pressure boundary surrounding the corners or edges of the reservoir model, ensuring that pressure remains fixed throughout the simulation process (Sun & Ertekin, 2019).

This study focuses on solving the diffusivity equation for a one-phase, one-dimensional reservoir system using a Cartesian grid and the Explicit Finite Difference Method (FDM). The primary objective is to determine the pressure distribution over time, specifically the value of p_i^{n+1} . A sensitivity analysis is conducted to evaluate the influence of several parameters on reservoir pressure, including grid spacing, time step, hydraulic diffusivity, no-flow boundaries, and boundary condition specifications.

The computational analysis is performed using MATLAB software, where a custom program is developed to estimate the pressure distribution, as illustrated in Figure 2 (see Appendices). Additionally, the flowchart of the study process is presented in Figure 3 (see Appendices), outlining the overall simulation workflow.

III. RESULTS AND DISCUSSIONS

This study presents a numerical simulation of a one-dimensional, single-phase Cartesian grid system. The simulation develops the diffusivity equation, also known as the partial differential equation (PDE), using the finite difference method as formulated in Equation (13). The pressure distribution for the new time level is calculated through the explicit finite difference method, as described in Equation (15). A sensitivity analysis is also included to evaluate the effects of various parameters on the reservoir's pressure behavior and overall performance. The reservoir model applied in this study, illustrated in Figure 4 (see Appendices), comprises six grid blocks representing the main reservoir and two additional boundary grid blocks positioned at the corners, modeled as fictitious grids. Two cases with distinct reservoir parameter values are analyzed to assess the influence of each factor on the simulation outcomes.

In Case 1, the reservoir is modeled using data from the base case synthesis simulation, as presented in Table 1 (see Appendices). Within this model, the flow rate is assumed to be zero in regions without well production or injection activity, and a no-flow boundary condition is applied to represent the closed boundaries of the reservoir. The reservoir properties consist of a porosity of 20 percent, permeability of 10 millidarcies (md), viscosity of 1 centipoise (cp), and a total compressibility of 5.0×10^{-6} . These parameters serve as the baseline conditions for evaluating pressure distribution and hydraulic diffusivity behavior across the grid system.

The reservoir in Case 1 has dimensions of 800 ft in length, divided into eight cells, with each cell occupying 100 ft along the coordinate axis. The simulation uses a time step of 0.05 days over a total duration of 10 days, with an initial reservoir pressure of 2500 psia at time zero (t = 0). The calculated stability value for this case is 0.316, confirming that the system is conditionally stable since the convergence criterion $\frac{\Delta t}{\Delta x}$ remains below than 0.5. This stability difference method produces reliable numerical results within the defined temporal and spatial discretization parameters.

Figures 5a and 5b (see Appendices) illustrate the relationship between pressure distribution and grid blocks at each time step, providing a clear depiction of how pressure evolves spatially within the reservoir. The results indicate a continuous decline in pressure over time, as shown in Figure 5c (see Appendices), which reflects the expected depletion behavior under

a no-flow boundary condition. In this configuration, the left boundary condition (BCL) corresponds to grid block 1, while the right boundary condition (BCR) is assigned to grid block 8, which maintains a pressure value of zero, signifying the boundary limit of the reservoir model.

In Case 2, the reservoir model incorporates a specified boundary condition, where the flow rate is assumed to be zero in zones without well production or injection activity. The reservoir parameters are defined with a porosity of 26 percent, permeability of 25 millidarcies (md), viscosity of 1.75 centipoise (cp), and a total compressibility of 7×10^{-6} . The reservoir extends 2000 ft in length and is discretized into 8 cells, with each cell measuring 250 ft along each coordinate axis. The simulation employs a time step of 10 days, and the initial reservoir pressure is set at 2500 psia at time zero (t = 0), establishing the baseline condition for the numerical analysis.

The stability analysis for Case 2 yields a value of 0.3975, confirming that the system is $\frac{\Delta t}{\Delta x^2 \gamma}$ < 0.5. stable since the convergence criterion $\frac{\Delta t}{\Delta x^2 \gamma}$ < 0.5. Figures 6a and 6b (see Appendices) illustrate the variation in pressure distribution across the grid blocks at successive time steps. As shown in Figure 6c (see Appendices), the reservoir pressure decreases progressively with increasing time steps, indicating a consistent pressure decline pattern. In this case, the BCL is defined at grid block 1, where the pressure is maintained at zero, while the BCR at grid block 8 corresponds to the initial reservoir pressure of 2500 psia.

This study incorporates a comprehensive sensitivity analysis to evaluate the influence of the reservoir model and its associated properties on pressure behavior. The analysis investigates multiple parameters, including grid length and spacing, the number of time steps, boundary conditions, porosity, permeability, viscosity, and compressibility. The data utilized in this analysis are derived from synthesized base case simulations, and the detailed outcomes are summarized in Table 2 (see Appendices).

The results of the sensitivity analysis indicate that variations in grid spacing significantly affect the pressure distribution within the reservoir, as seen in Table 3 (see Appendices). As illustrated in Figure 7a (see Appendices), longer grid lengths produce pressure distributions that increase and tend to approach the initial pressure. The effect of time-step variations, shown in Figure 7b (see Appendices), demonstrates that smaller time steps result in a higher pressure response. Meanwhile, Figure 7c (see Appendices) depicts the influence of the BCL, where lower pressure at the boundary induces a continuous pressure decline over time.

In addition, the sensitivity analysis of reservoir parameters, as illustrated in Figures 8a, 8b, 8c, and 8d (see Appendices), shows that higher porosity, viscosity, and compressibility contribute to an overall increase in total pressure yield over time, thereby affecting the reservoir's pressure profile. Conversely,

as demonstrated in Figure 8b (see Appendices), reservoirs with higher permeability values exhibit a decrease in pressure over time. These findings confirm the strong dependence of pressure behavior on both geometric and petrophysical reservoir characteristics, highlighting the complex interplay between grid configuration, fluid properties, and flow dynamics.

This study presents a numerical solution for stability analysis designed to approximate the analytical solution of the diffusivity equation. The convergence of the solution depends on several parameters, including reservoir properties, grid dimensions, and time step size, all of which play a critical role in determining the optimal pressure distribution. For the explicit finite difference method to maintain conditional stability, the condition $\alpha = \left(\frac{\Delta t}{\Delta x^2 \gamma}\right) < 0.5$ must be satisfied. This requirement

ensures that the numerical solution remains accurate and free from divergence during computation. Two examples are presented to illustrate the process and implications of instability analysis in the context of reservoir simulation.

In the first example, the simulation uses data parameters consisting of a grid spacing of 75 ft, a time step of 0.008 days, a porosity of 0.15, a viscosity of 0.45 cp, a total compressibility of 1.5×10^{-6} 1/psi, and a permeability of 7 md. These parameters produce an α value of 0.6224 and a hydraulic diffusivity (γ) of 2.285 \times 10⁻⁶. As illustrated in Figure 9 (see Appendices), instability occurs at time steps t = 3 and t = 4, corresponding to the point where α exceeds the threshold of 0.5. This finding confirms that the explicit finite difference scheme becomes unstable when the stability condition is violated, leading to divergence in the pressure solution.

The second example applies a specified boundary condition on the left side with a pressure of 2500 psi. The simulation uses data parameters including a grid spacing of 100 ft, a time step of 0.05 days, a porosity of 0.26, a viscosity of 15 cp, a total compressibility of 2.5×10^{-6} 1/psi, and a permeability of 15 md. This parameters yields an α value of a = 0.6351 and a hydraulic diffusivity (γ) of 7.872×10^{-6} . As shown in Figure 10 (see Appendices), instability is observed at time steps t = 3 and t = 4, consistent with the findings from the first example. This result further confirms that instability arises when α exceeds 0.5, validating the conditionally stable nature of the explicit finite difference scheme in the stability analysis.

IV. CONCLUSIONS

This study investigates the numerical simulation of a petroleum reservoir system modeled as a single-phase, one-dimensional Cartesian grid. It employs the explicit finite difference method to solve the diffusivity equation, offering a practical and efficient approach commonly utilized in the petroleum industry for reservoir modeling and performance prediction.

The analysis focuses on determining the pressure distribution under both no-flow and specified boundary conditions, as well as identifying reservoir parameters that significantly influence pressure distribution and system stability. This approach provides valuable insights into the dynamic behavior of fluid flow in porous media.

The findings demonstrate that variations in reservoir characteristics lead to distinct pressure responses. An increase in grid spacing, porosity, viscosity, compressibility, and boundary condition values generally corresponds to higher total pressure, whereas greater permeability results in lower pressure. Furthermore, smaller time steps tend to produce a more significant pressure drop, indicating a sensitivity of the system to temporal resolution. The stability analysis confirms that convergence improves with adjustments in the α parameter and hydraulic diffusivity (γ), reinforcing the reliability of the explicit finite difference method in simulating transient reservoir behavior.

In summary, this research contributes to a better understanding of pressure distribution and flow performance in petroleum reservoir systems. The explicit finite difference method demonstrates conditional stability and computational efficiency, providing a consistent framework for analyzing reservoir dynamics. The validated analytical results affirm the accuracy of this numerical approach, supporting its use in practical engineering applications. Future work will expand on this foundation by developing the implicit finite difference method to improve numerical stability and comparing the results with commercial reservoir simulation software to enhance the accuracy of predictive reservoir modeling.

ACKNOWLEDGEMENT

The authors acknowledge the Department of Petroleum Engineering at Universitas Trisakti for the financial support that made this research possible and is reported in this paper. Furthermore, the author would like to thank Zuher Syihab, Ph.D., for his expertise in numerical simulation, which enabled the creation of this research.

AUTHOR CONTRIBUTIONS

Conceived and designed the analysis, S. F. M.; Collected the data, S. F. M., A. P., J. A. W., P. R. and H. W.; Contributed data or analysis tools, S. F. M., A. P., J. A. W., P. R. and H. W.; Performed the analysis, S. F. M., A. P., J. A. W., P. R. and H. W.; Wrote the paper, S. F. M., A. P., J. A. W., P. R. and H. W.; Implicit method comparison, A. P.; Adding formula diffusivity equation, J. A. W.; Provide input regarding between the specified boundary condition, P. R.; Provide input regarding between the specified boundary condition, H. W.

DATA AVAILABILITY

The data were generated from laboratory reservoir simulations at Universitas Trisakti. Additional data supporting the findings of this study are available upon request from the corresponding author, Maulindani.

REFERENCES

- Abou-Kassem, J. H., Islam, M. R., & Farouq Ali, S. M. (2020). Chapter 4 Simulation with a block-centered grid. In J. H. Abou-Kassem, M. R. Islam, & S. M. Farouq Ali (Eds.), *Petroleum Reservoir Simulation (Second Edition)* (Second Edi, pp. 65–124). Gulf Professional Publishing. https://doi.org/10.1016/B978-0-12-819150-7.00004-9
- Adak, M. (2020). Comparison of explicit and implicit finite difference schemes on diffusion equation. *Springer Proceedings in Mathematics and Statistics*, 320, 227–238. https://doi.org/10.1007/978-981-15-3615-1 15
- Aliyu, B. K., Agency, D., Olatoyinbo, S. F., Agency, D., & Vehicle, U. A. (2021). *Explicit and Implicit Solution to 2D Heat Equation. February*. https://doi.org/10.13140/RG.2.2.10788.19840
- Appau, P. O., Dankwa, O. K., & Brantson, E. T. (2019). A comparative study between finite difference explicit and implicit method for predicting pressure distribution in a petroleum reservoir. *International Journal of Engineering, Science and Technology*, 11(4), 23–40. https://doi.org/10.4314/ijest.v11i4.3
- Contreras, F. R. L., Carvalho, D. K. E., Galindez-Ramirez, G., & Lyra, P. R. M. (2021). A nonlinear finite volume method coupled with a modified higher order MUSCL-type method for the numerical simulation of two-phase flows in non-homogeneous and non-isotropic oil reservoirs. *Computers and Mathematics with Applications*, *92*, 120–133. https://doi.org/10.1016/j.camwa.2021.03.023
- Galindez-Ramirez, G., Contreras, F. R. L., Carvalho, D. K. E., & Lyra, P. R. M. (2020). Numerical simulation of two-phase flows in 2-D petroleum reservoirs using a very high-order CPR method coupled to the MPFA-D finite volume scheme. *Journal of Petroleum Science and Engineering*, 192, 107220. https://doi.org/10.1016/j.petrol.2020.107220
- Ghedira, A., Lataoui, Z., Benselama, A. M., Bertin, Y., & Jemni, A. (2025). Numerical simulation of incompressible two-phase flows with phase change process in porous media. *Results in Engineering*, 25, 103706. https://doi.org/10.1016/j.rineng.2024.103706
- Keita, S., Beljadid, A., & Bourgault, Y. (2021). Efficient second-order semi-implicit finite element method for fourth-order nonlinear diffusion equations. *Computer Physics Communications*, 258, 107588. https://doi.org/10.1016/j.cpc.2020.107588

- Kvashchuk, A., Klöfkorn, R., & Sandve, T. H. (2023). A second-order finite volume method for field-scale reservoir simulation. *Transport in Porous Media*, 150(1), 109–129. https://doi.org/10.1007/s11242-023-01999-1
- Liu, H., & Luo, Y. (2022). An explicit method to calculate implicit spatial finite differences. *Geophysics*, 87(2), T157–T168. https://doi.org/10.1190/geo2021-0001.1
- Maulindani, S. F., Abdassah, D., Marhaendrajana, & Prakoso, S. (2021). Reservoir simulation study for dual porosity model to determine characteristic of naturally fractured reservoir. 3rd International Conference on Earth Science, Mineral, and Energy, 2363, 020006. https://doi.org/10.1063/5.0061130
- Maulindani, S. F., Abdassah, D., Marhaendrajana, T., Prakoso, S., & Fathaddin, M. T. (2021). Application of pressure type curve matching for characterizing the naturally fractured reservoir. *Journal of Earth Energy Science, Engineering, and Technology*, 4(1). https://doi.org/10.25105/jeeset.v4i1.9060
- Mojumder, M. S. H., Haque, M. N., & Alam, M. J. (2023). Efficient finite difference methods for the numerical analysis of one-dimensional heat equation. *Journal of Applied Mathematics and Physics*, *11*(10), 3099–3123. https://doi.org/10.4236/jamp.2023.1110204
- Nascimento, J. C. S., Santos, A. dos, Pico Ortiz, C. E., & Pires, A. P. (2021). A fully implicit EOS based compositional two-phase transient flow simulator

- in wellbores. *Journal of Petroleum Science and Engineering*, 205(May). https://doi.org/10.1016/j.petrol.2021.108923
- Raza, Q., & Wang, X. (2024). Numerical simulation of Boger nanofluids with heat source, magnetic field, and Cattaneo–Christov heat flux model between two parallel permeable porous plates via finite difference method. *Case Studies in Thermal Engineering*, 64(May), 105518. https://doi.org/10.1016/j.csite.2024.105518
- Salomon, L., & Guilcher, P. M. (2024). Fully higher-order coupling of finite element and level set methods for two-phase flow with a new explicit projection method. *Computers and Fluids*, 275(February), 106245. https://doi.org/10.1016/j.compfluid.2024.106245
- Sun, Q., & Ertekin, T. (2019). *Reservoir Simulation: Problems and Solutions*. https://doi.org/10.2118/9781613996935
- Sun, Q., Zhang, R., Zhan, Q., Member, S., & Liu, Q. H. (2019). 3-D implicit – explicit hybrid finite difference / spectral element / finite element time domain method. *IEEE Transactions on Antennas* and Propagation, 67(8), 5469–5476.
- Wang, S., Yu, C., Sang, G., Yu, R., & Cheng, F. (2020). An oil water two-phase reservoir numerical simulation coupled with dynamic capillary force based on the full-implicit method. *Computers and Mathematics with Applications*, 79(9), 2527–2549. https://doi.org/10.1016/j.camwa.2019.11.013

APPENDICES

Table 1 Base Case Synthesis Simulation Data

Reservoir Parameter	Value	Unit	
Pressure initial	2500	Psia	
Porosity	20	Percent	
Permeability	10	md	
Compressibility total	2.8	1/psia	
Viscosity	1		
Reservoir model			
Grid spacing	100	ft	
Time step	0.005	days	
No-flow boundary	0	Psia	
Boundary Left/ Right	2500	Psia	

Table 2 Numerical Simulation Case

Properties	Case 1	Case 2						
Reservoir model								
Grid spacing, ft	100	250						
Time step, days	0.05	0.5						
Hydraulic Diffusivity Parameter								
Porosity, %	20	26						
Permeability, md	10	25						
Viscosity, cp	1	1.75						
Compressibility total, 1/psi								
Boundary condition								
No-flow boundary	0	0						
Specified boundary conditions	0	PBCL = 0 PBCR = Initial Pressure						

Table 3 Sensitivity Analysis Case

Reservoir Model								
Grid spacing, ft	100	200	300	400	500			
Time step, days	0.0025	0.005	0.01	0.025	0.05			
Hydraulic Diffusivity Parameter								
Porosity, %	20	22	24	26	28			
Permeability, md	10	20	25	30	35			
Viscosity, cp	1. 0	1.5	1.75	2	2.25			
Compressibility total, 1/psi		4.0	5.0	6.0	7.0			
Boundary Condition								
Presence of boundary conditions =BCL	2500	2250	1500	1250	500			

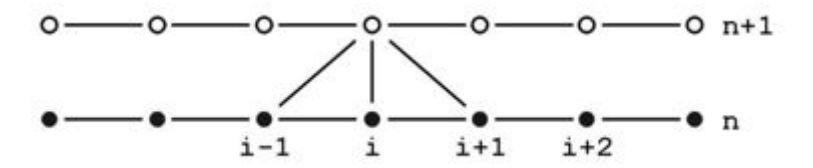


Figure 1 Schematic solution using the Explicit Method

```
& Explicit method for finite different second derivative for diffusivity
  % Equation for 1D dimension and single phase oil
  % Dimension of grid cartesian
  Nx = 8; % number of grid, ft
  Nt = 10; % number of time step, days
  % Reservoir properties
  por=0.20; % value of porosity , fraction
  mio = 1.0; % value of visocosity, cp
  ct = 5.0E-06; % value of compressibility, 1/psi
  perm = 10; % value of permeability, mD
  Dt = 0.05; % time step, days
  Dx = 100; % length of grid, ft
  % calculating hydraulic diffusivity
 lamda = (por*mio*ct)/(0.00633*perm);
  %calculating alpha
  alpha = Dt/(lamda*Dx.^2);
  * Estimating for Initial Condition and Boundary Condition
  P = zeros(Nt, Nx);
  P(1,2:Nx)=2500;% initial pressure at t=0
  P(:,1)=0;% left boundary condition
  P(:, Nx)=0; % right boundary condition
  * calculating using explicit method
for k = 1:Nt-1 % time loop
     for i = 2:Nx-1 % space loop
          P(k+1,i) = alpha*P(k,i+1) + (1-2*alpha)*P(k,i) + alpha*P(k,i-1);
      end
 end
  P % display the result of pressure distribution
  figure (1)
  t = 1:1:10;
  GB = 1:1:8;
 % plot (GB, P)
  plot(GB,P(1,:),'-b',GB,P(2,:),'--g',GB,P(Nt,:),'-.r','markersize',2,'linewidth',1.5)
  title ('Pressure Distribution')
  xlabel('gridblock')
  ylabel ('Pressure (psia)')
  legend('t=0','t=2','t=10')
  grid on
```

Figure 2 The Program code for this study in MATLAB

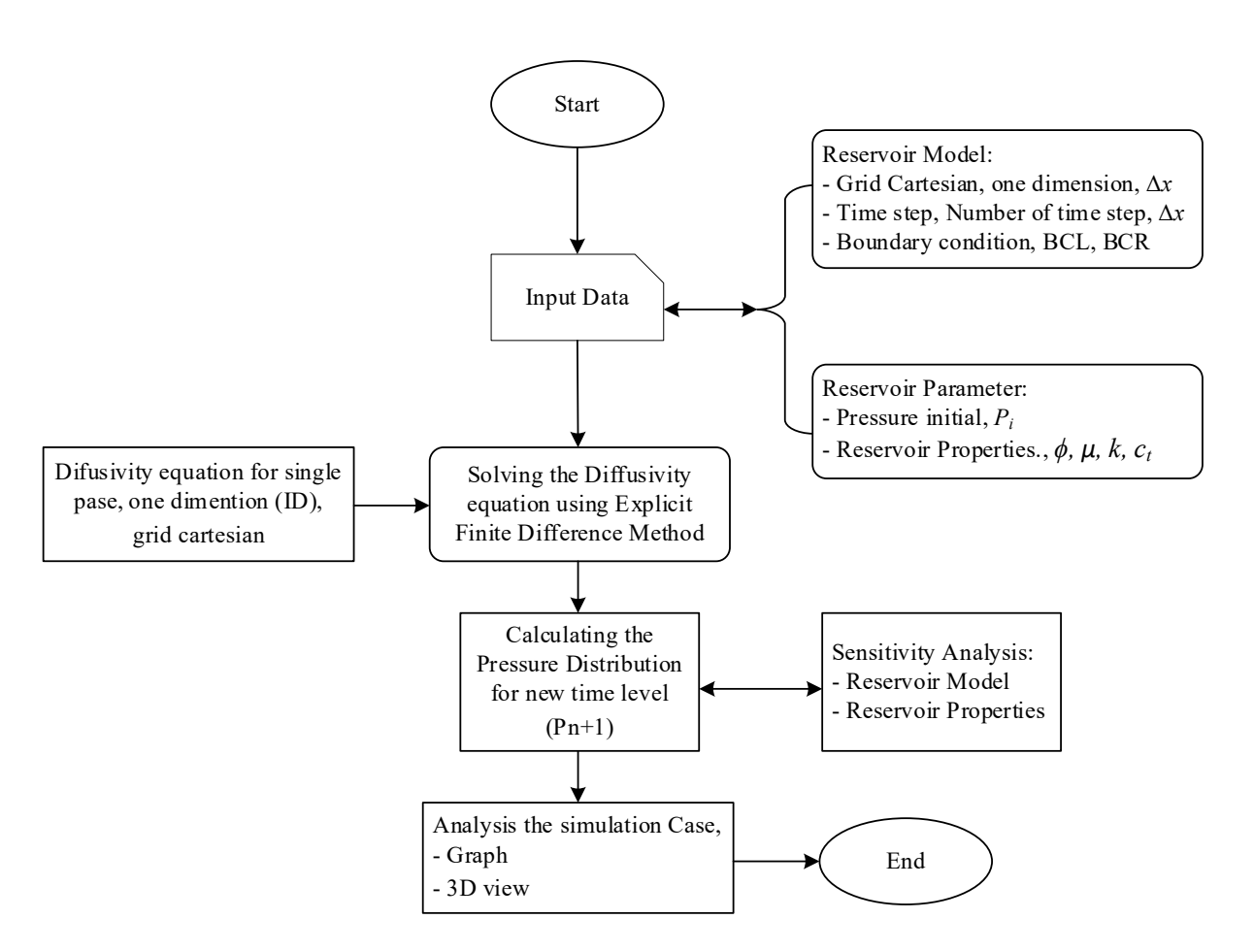


Figure 3 Flow Chart of Numerical Simulation Study

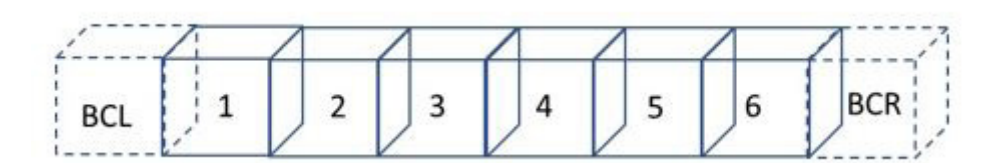
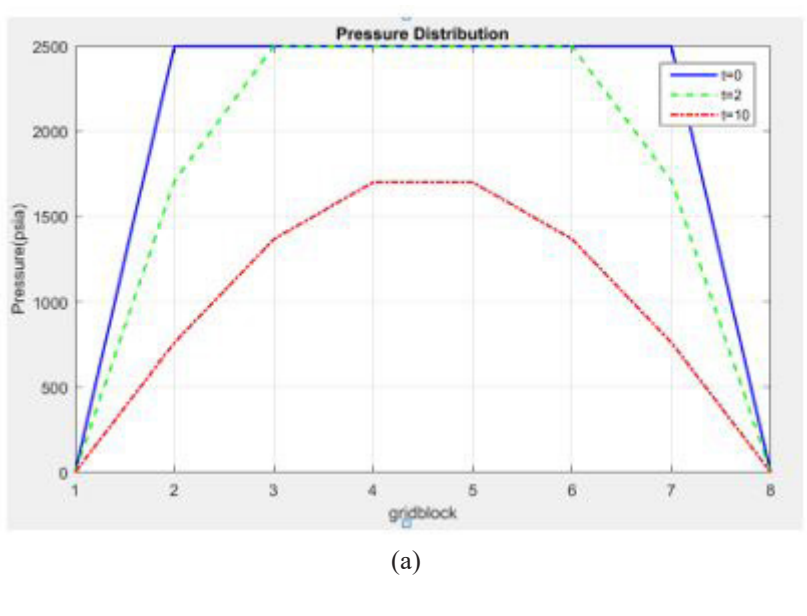
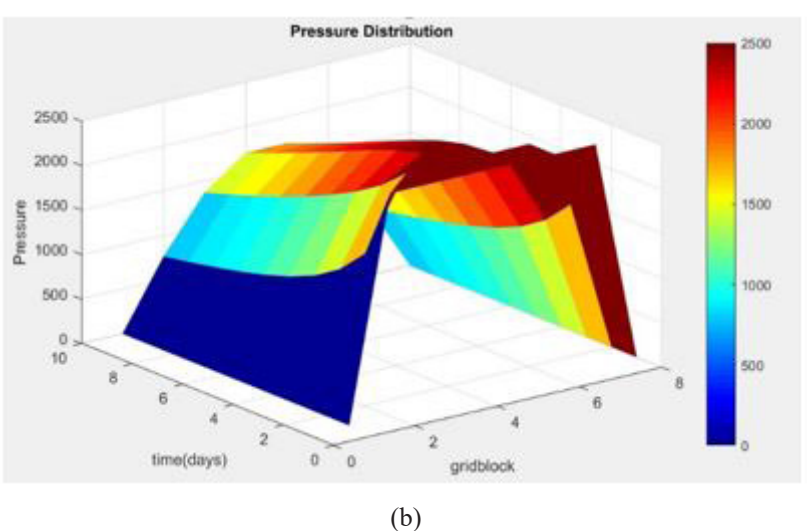


Figure 4 Reservoir Model Grid Cartesian with Boundary Condition





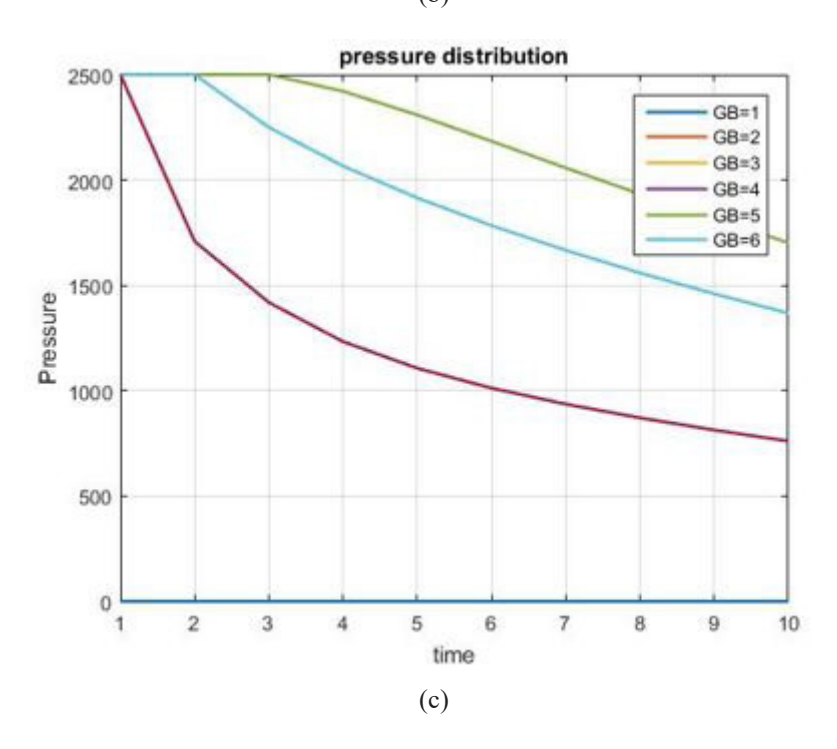
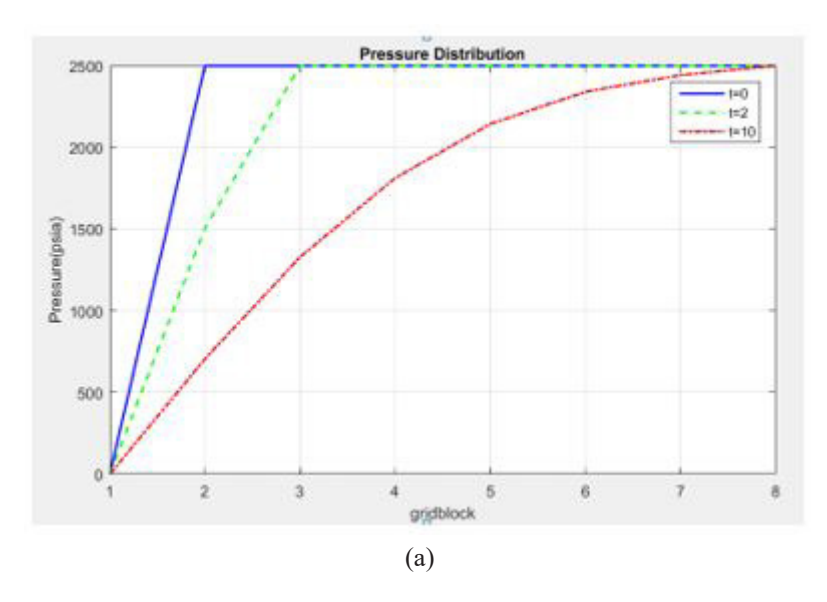
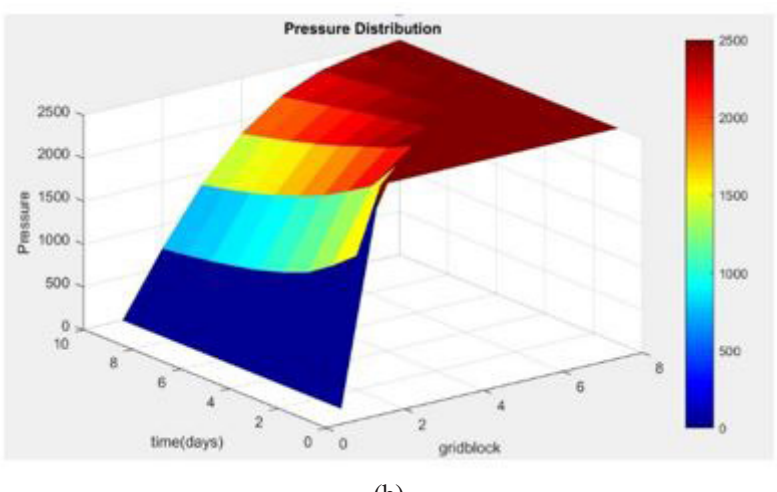


Figure 5 Pressure Distribution and mesh plot for Explicit scheme with no-flow boundary in (a),(b), and (c) are presented, for case 1 with $\alpha=0.3165$, $D_x=100$, and $D_t=0.05$

164





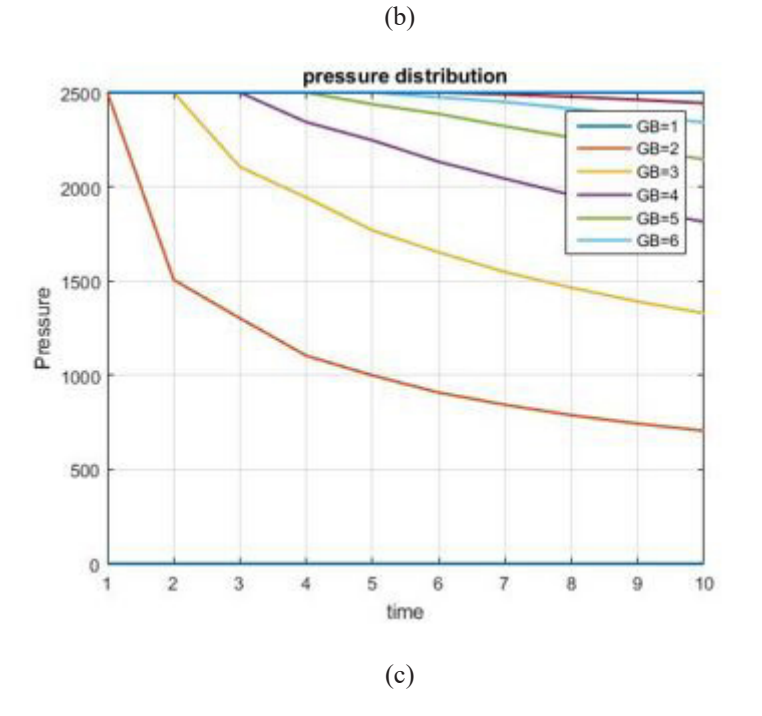
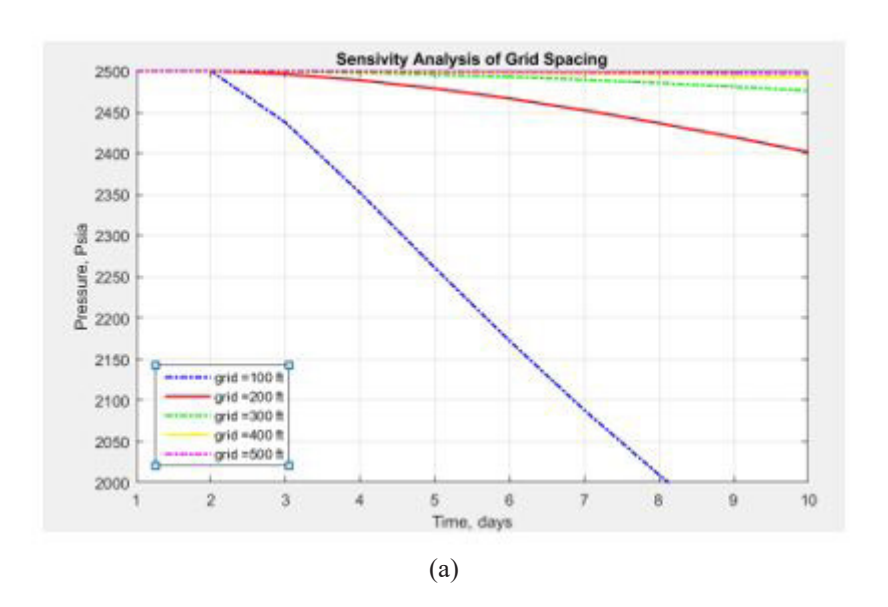
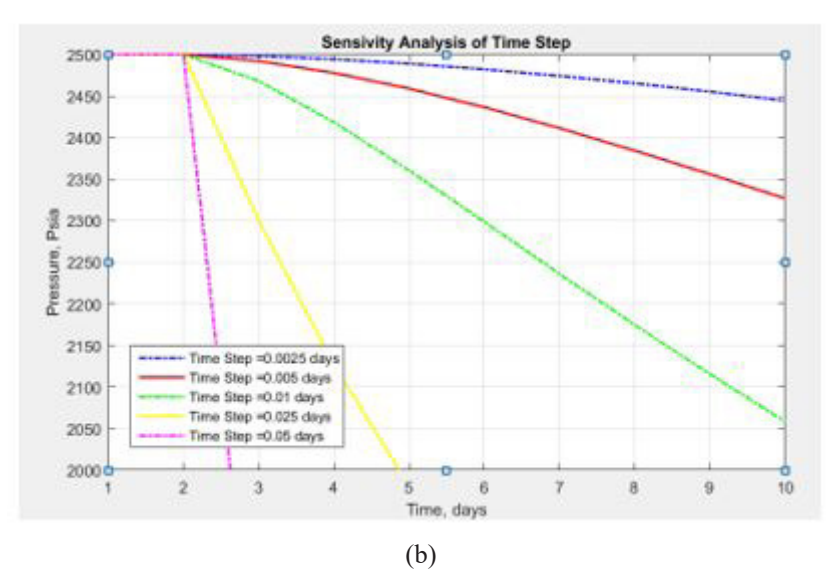


Figure 6 Pressure Distribution and mesh plot for Explicit scheme with Specify boundary condition = 2500 psi in (a),(b), and (c) are presented, for case 2 with $\alpha=0.3975$, $D_{_{X}}=250$, and $D_{_{t}}=0.5$





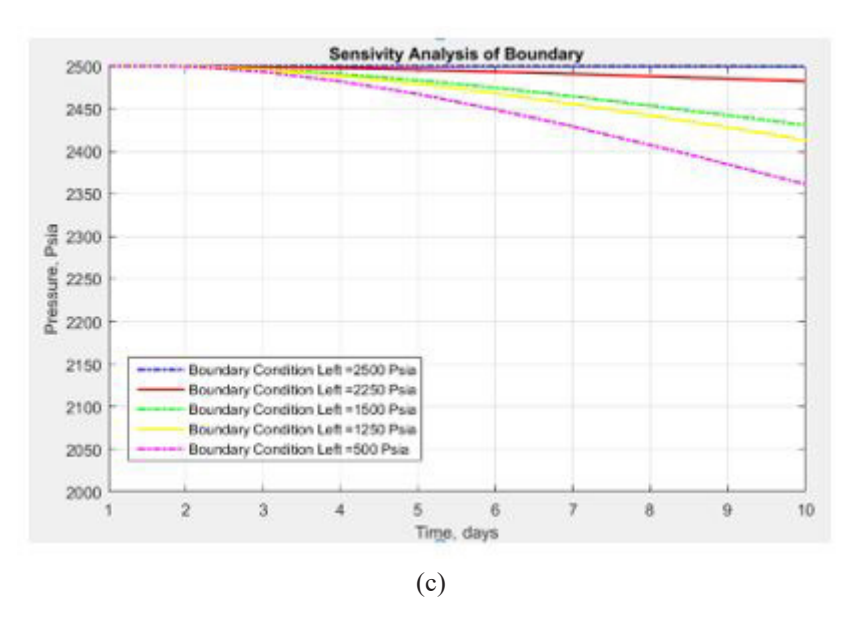


Figure 7 Pressure Distribution for Sensitivity Analysis of Reservoir Model (a), (b), and (c) are presented, for (a) a variety of grid spacing, (b) a variety of time steps, and (c) a variety of boundary conditions

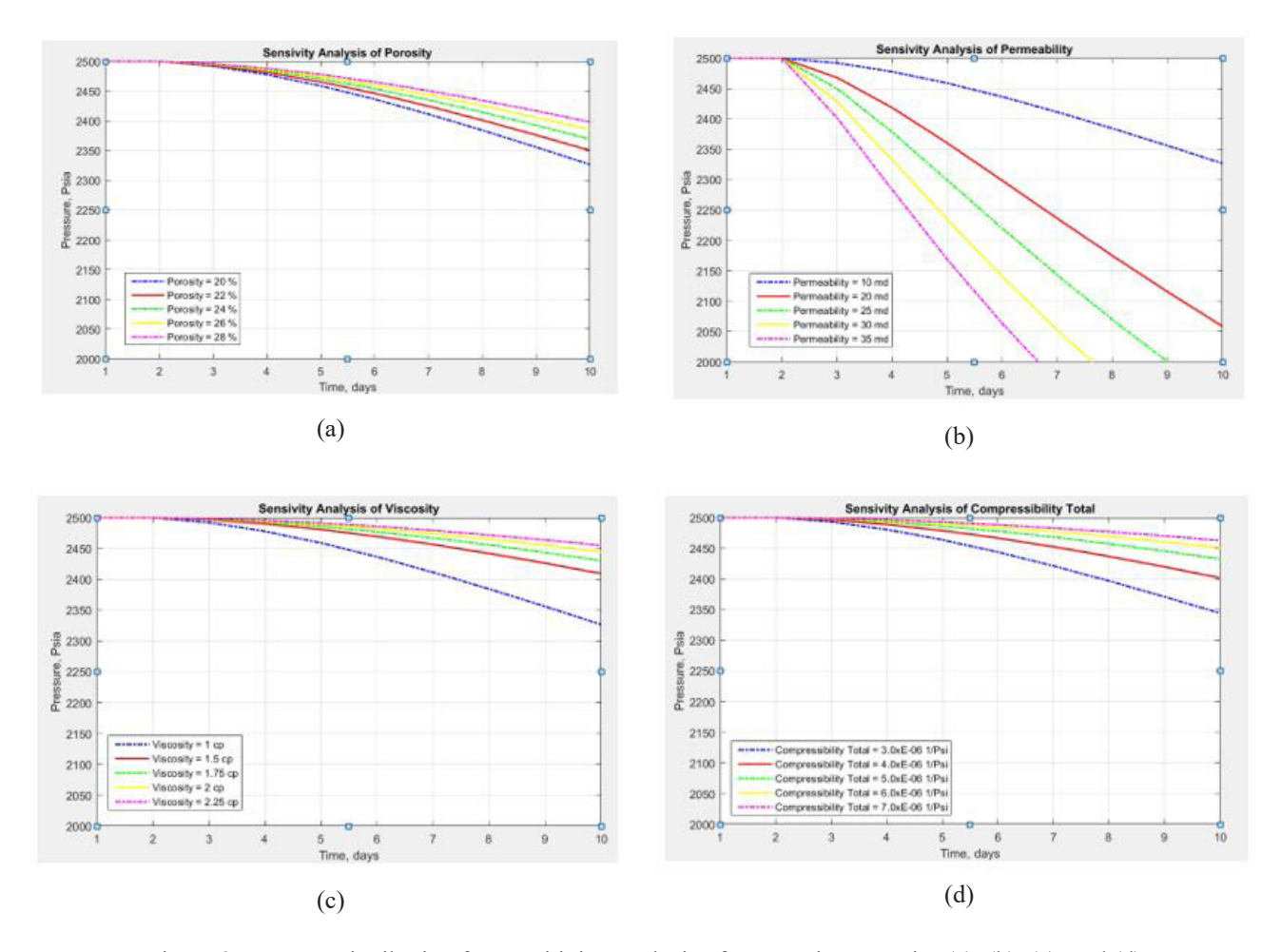


Figure 8 Pressure Distribution for Sensitivity Analysis of Reservoir Properties (a), (b), (c), and (d) are presented, for (a) a variety of porosity, (b) a variety of permeability, (c) a variety of viscosity, and (d) a variety of compressibility

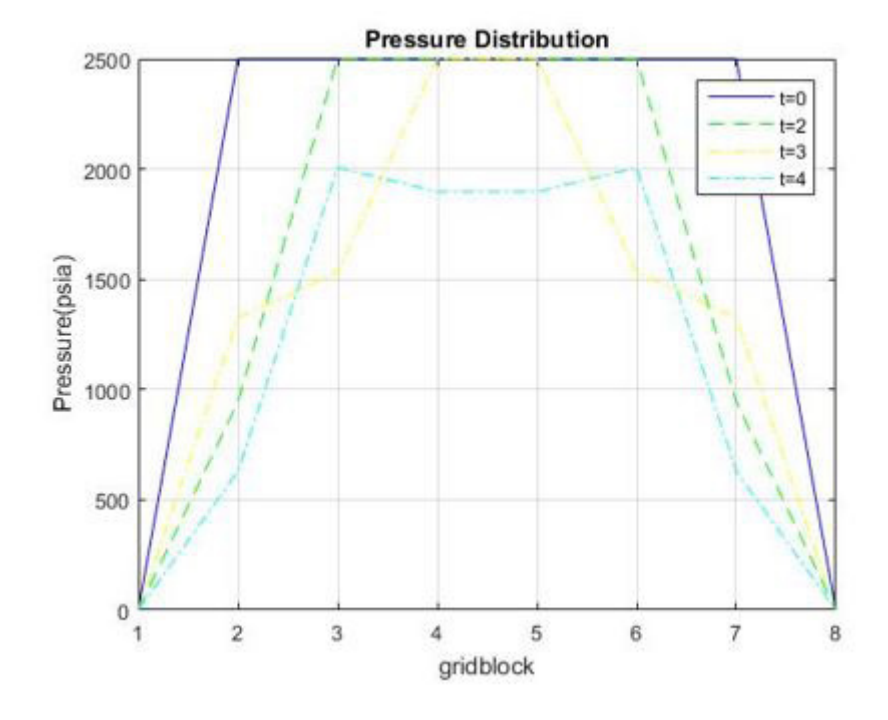


Figure 9 Unstability for Explict Scheme Example 1 with $\alpha=0.6224$, $\gamma=2.258\times10^{-6}, D_t=0.008$ days, and $D_x=75$ ft

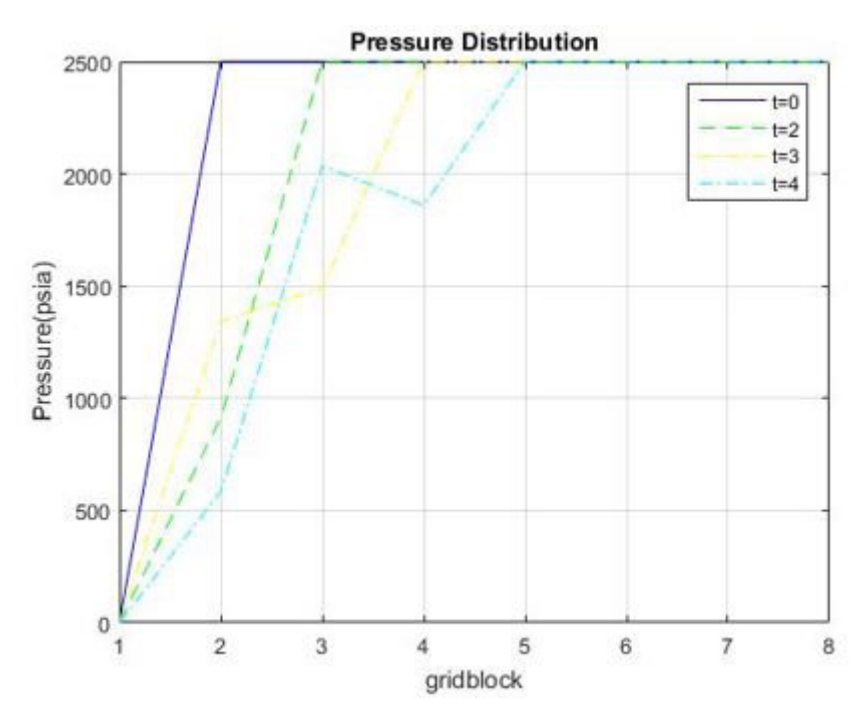


Figure 10 Unstability for Explict Scheme Example 2 with $~\alpha=0.6351,~\gamma=2.284\times10^{-6},~D_{t}=0.05$ days, and $D_{x}=100$ ft